NASA-CR-192369

AN EXPERIMENTAL STUDY OF GROWTH AND PHASE CHANGE OF POLAR STRATOSPHERIC CLOUD PARTICLES

Semiannual Status Report
Period covered: July 1 - December 31, 1991

NASA Research Grant NAG-W-2572

John Hallett
Principal Investigator

and M.S. Student: Edward Teets

Desert Research Institute
University of Nevada System
P.O. Box 60220
Reno, Nevada 89506-0220

March 1992

Semiannual NASA report

"An Experimental Study of Growth and Phase Change of Polar Stratospheric Cloud Particles"

By John Hallett and
M.S. Student: Edward Teets

This reports progress made on understanding phase changes related to solutions which may comprise Polar Stratospheric Clouds. In particular, it is concerned with techniques for investigating specific classes of metastability and phase change which may be important not only in Polar Stratospheric Clouds but in all atmospheric aerosol in general. While the lower level atmospheric aerosol consists of mixtures of $(NH_4)(SO_4)_2$, NH_4HSO_4, NaCl among others, there is evidence that aerosol at PSC levels is composed of acid aerosol, either injected from volcanic events (such as Pinatubo) or having diffused upward from the lower atmosphere. In particular, sulfuric acid and nitric acid are known to occur at PSC levels, and are suspected of catalyzing ozone destruction reactions by adsorption on surfaces of crystallized particles. Such particles may result from water absorption by the acid aerosol followed by crystallization as hydrates or ice depending on temperature and composition.

A major question arises as to the extent to which such particles supercool (supersaturate) prior to crystallization, the nature of the crystallization itself in these droplets, and the nature of subsequent growth from the vapor of crystals in the form of ice or hydrate depending on the environmental conditions - temperature or vapor pressure (relative humidity). A crucial first question is the occurrence of solutions which supersaturate. It is well known (see Mason, The Physics of Clouds 1970) that aerosol particles in the lower atmosphere, of composition listed above, supersaturate substantially and

contribute to a hysteresis in visibility. The amount and time dependence of such metastability is ill understood, as is the dependence on insoluble aerosol (particularly soot) to nucleate such metastable particles, (Hallett, 1991). Identical questions occur for stratospheric clouds. The present study has centered on two approaches:

1) The extent of supercooling (with respect to ice) and supersaturation (with respect to hydrate) and the nature of crystal growth in acid solutions of specific molality.

2) The nature of growth from the vapor of HNO_3 - H_2O crystals both on a substrate and on a pre-existing aerosol.

1. Techniques:

The first class of experiment is designed to explore the range of supercooling (i.e. with respect to ice phase nucleation) of acid solutions of different concentration and temperatures down to -90°C. This was accomplished by observing cooling curves of approximately 1 ml solution in a glass test tube cooled slowly through the appropriate temperature of metastability. In practice, the approximate freezing (nucleation) point of each solution is determined; the final measurements were made for samples cooled rapidly to about 10°C above the expected nucleation temperature, then cooled slowly (1/100°C s^{-1}) until nucleation occurred. Such nucleation was readily detected by a sudden increase of solution temperature by latent heat release (Fig. 1). The nucleation was visible as ice crystals propagating through the solution. To each molality solution there is assigned an equilibrium freezing point depression (Table 1, 2). Above this temperature an inserted ice crystal will melt; below this temperature an inserted ice crystal will grow. This defines the concept of equilibrium freezing point, Figures 2, and 3 show the maximum supercooling obtained for

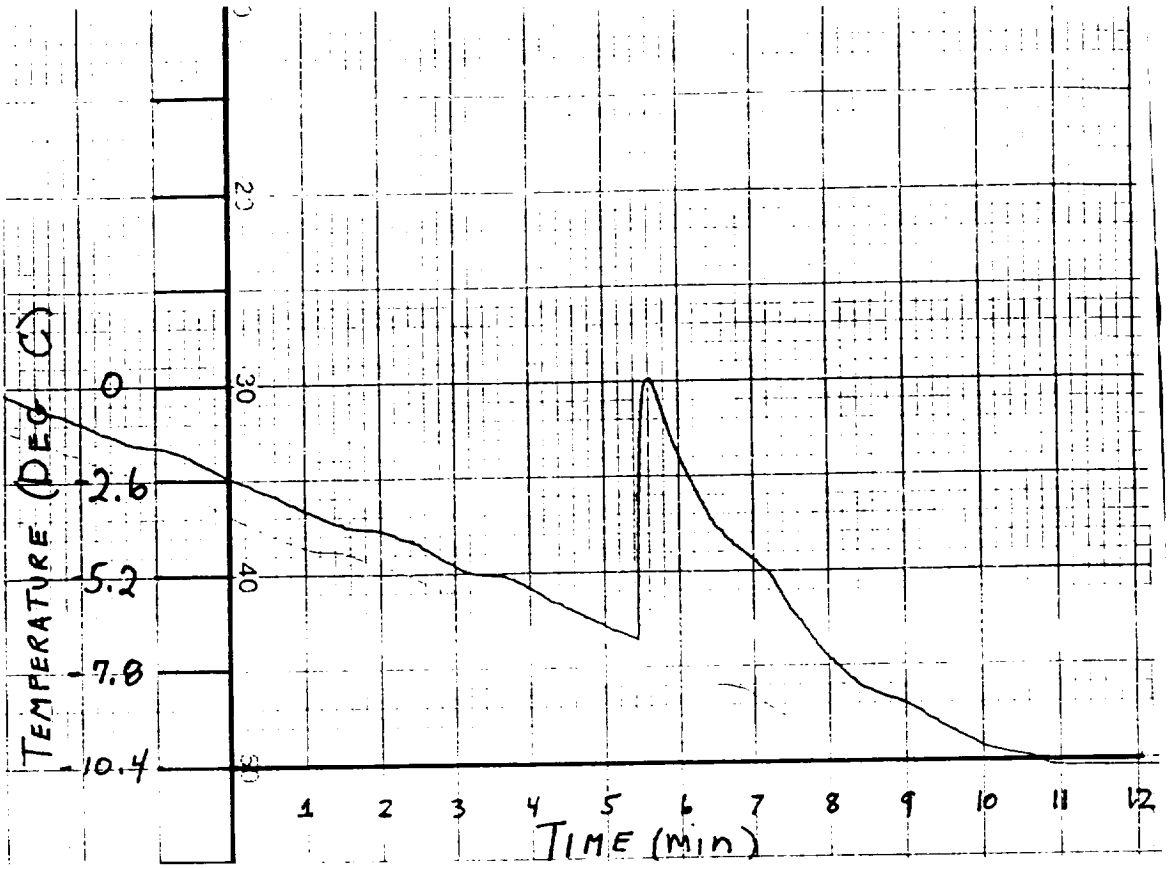

Figure 1(a) Cooling curve of 1 ml pure liquid water, showing the point of maximum supercooling and equilibrium freezing temperature.

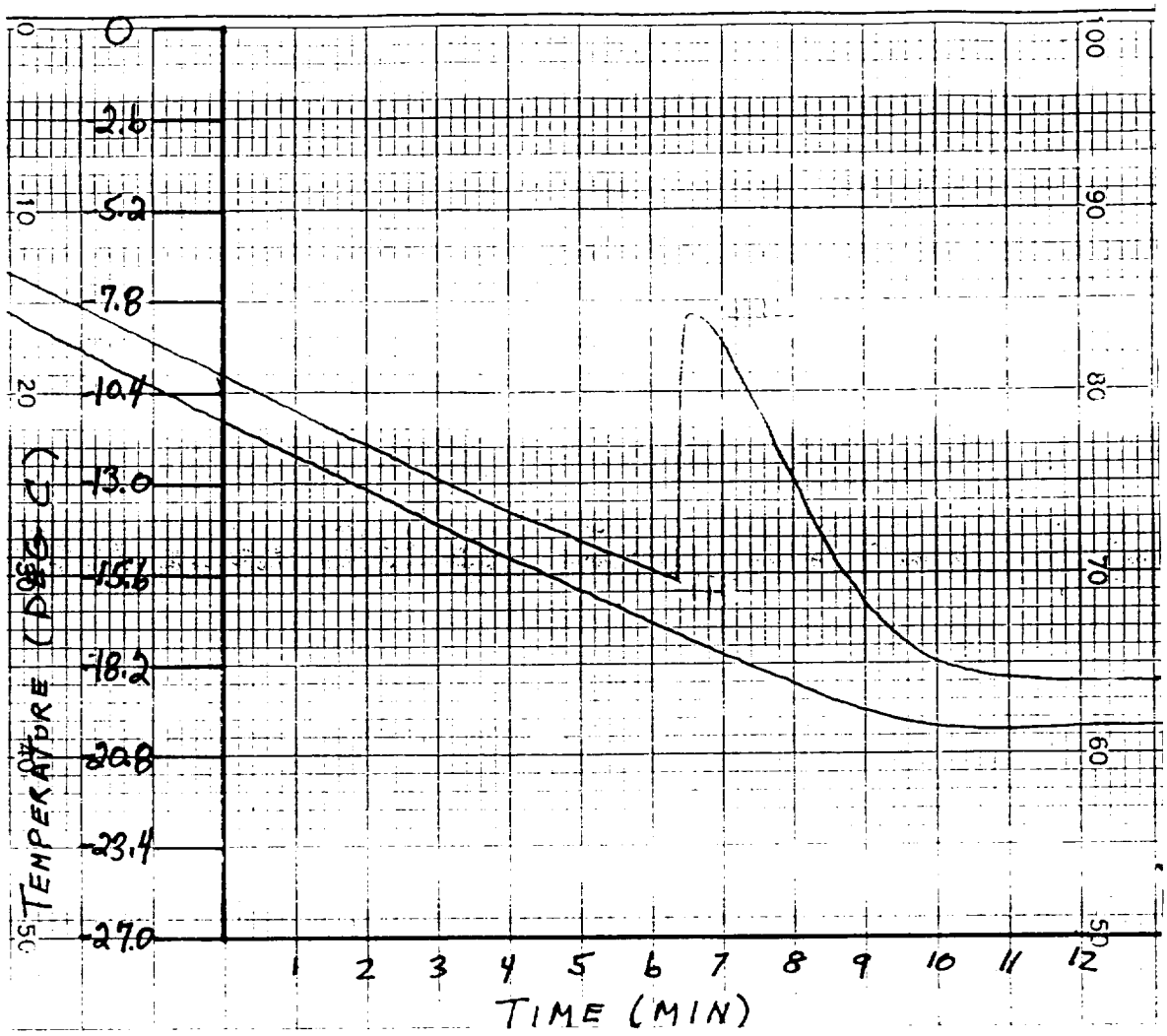

Figure 1(b). Same as Figure 1(a) but, for 1 m HNO_3 solution.

Table 1 From Chemistry and Physics Handbook.

89 SULFURIC ACID, H_2SO_4

MOLECULAR WEIGHT = 98.08
RELATIVE SPECIFIC REFRACTIVITY = 0.685

0.00 % by wt. data are the same for all compounds.
For Values of 0.00 wt. % solutions see Table 1, Acetic Acid.

A % by wt	ρ D_4^{20}	D_4^{25}	C_1 g/l	M g-mol/l	C_2 g/l	$(C_2 - C_1)$ g/l	$(n - n_1)$ $\times 10^4$	n	Δ °C	O OS/kg	S g-mol/l	η cP	η/ρ cS	ϕ rhe	γ mmho/cm	T g-mol/l
0.50	1.0016	1.0034	5.0	0.051	996.6	1.7	6	1.3336	0.210	0.113	0.060	1.008	1.009	98.96	24.3	0.277
1.00	1.0049	1.0067	10.0	0.102	994.9	3.3	13	1.3342	0.423	0.227	0.122	1.017	1.014	98.13	47.8	0.573
1.50	1.0083	1.0101	15.1	0.154	993.2	5.1	19	1.3349	0.662	0.356	0.192	1.025	1.019	97.34	70.3	0.886
2.00	1.0116	1.0134	20.2	0.206	991.4	6.8	25	1.3355	0.796	0.428	0.232	1.034	1.024	96.52	92.	1.22
2.50	1.0150	1.0168	25.4	0.259	989.6	8.6	31	1.3361	1.004	0.540	0.293	1.044	1.031	95.55	113.	1.58
3.00	1.0183	1.0201	30.6	0.311	987.8	10.4	37	1.3367	1.172	0.630	0.343	1.057	1.040	94.45	134.	1.98
3.50	1.0217	1.0235	35.8	0.365	985.9	12.3	43	1.3373	1.354	0.728	0.396	1.070	1.049	93.29	155.	2.42
4.00	1.0250	1.0269	41.0	0.418	984.0	14.2	49	1.3379	1.599	0.860	0.468	1.083	1.059	92.11	175.	2.93
4.50	1.0284	1.0302	46.3	0.472	982.1	16.1	55	1.3385	1.855	0.998	0.543	1.097	1.069	90.97	194.	3.57
5.00	1.0318	1.0336	51.6	0.526	980.2	18.0	61	1.3391	2.047	1.101	0.598	1.110	1.078	89.91	211.	4.25
5.50	1.0352	1.0370	56.9	0.580	978.2	20.0	67	1.3397	2.259	1.214	0.659	1.122	1.086	88.93		
6.00	1.0385	1.0404	62.3	0.635	976.2	22.0	73	1.3403	2.495	1.341	0.727	1.134	1.094	88.00		
6.50	1.0419	1.0438	67.7	0.691	974.2	24.0	79	1.3409	2.730	1.468	0.795	1.146	1.102	87.10		
7.00	1.0453	1.0472	73.2	0.746	972.2	26.1	85	1.3415	2.952	1.587	0.858	1.157	1.109	86.24		
7.50	1.0488	1.0506	78.7	0.802	970.1	28.1	91	1.3421	3.197	1.719	0.927	1.169	1.117	85.39		
8.00	1.0522	1.0541	84.2	0.858	968.0	30.2	97	1.3427	3.493	1.878	1.010	1.180	1.124	84.56		
8.50	1.0556	1.0575	89.7	0.915	965.9	32.3	103	1.3433	3.801	2.043	1.096	1.192	1.131	83.74		
9.00	1.0591	1.0610	95.3	0.972	963.8	34.4	109	1.3439	4.083	2.195	1.174	1.204	1.139	82.92		
9.50	1.0626	1.0645	100.9	1.029	961.6	36.6	115	1.3445	4.360	2.344	1.250	1.216	1.146	82.10		
10.00	1.0661	1.0680	106.6	1.087	959.5	38.8	121	1.3451	4.644	2.497	1.328	1.228	1.154	81.27		
11.00	1.0731	1.0750	118.0	1.204	955.1	43.2	133	1.3463	5.25	2.82	1.490	1.253	1.170	79.63		
12.00	1.0802	1.0821	129.6	1.322	950.6	47.6	145	1.3475	5.93	3.19	1.669	1.279	1.187	78.02		
13.00	1.0874	1.0893	141.4	1.441	946.0	52.2	158	1.3488	6.67	3.59	1.859	1.306	1.203	76.43		
14.00	1.0947	1.0966	153.3	1.563	941.4	56.8	170	1.3500	7.49	4.03	2.063	1.334	1.221	74.82		
15.00	1.1020	1.1039	165.3	1.685	936.7	61.5	183	1.3513	8.35	4.49	2.270	1.364	1.240	73.17		
16.00	1.1094	1.1114	177.5	1.810	931.9	66.3	195	1.3525	9.26	4.98	2.483	1.396	1.261	71.47		
17.00	1.1169	1.1189	189.9	1.936	927.0	71.2	208	1.3538	10.23	5.50	2.702	1.431	1.284	69.74		
18.00	1.1245	1.1265	202.4	2.064	922.1	76.2	221	1.3551	11.29	6.07	2.932	1.467	1.308	68.01		
19.00	1.1321	1.1341	215.1	2.193	917.0	81.2	233	1.3563	12.43	6.68	3.169	1.505	1.332	66.32		
20.00	1.1398	1.1418	228.0	2.324	911.9	86.4	246	1.3576	13.64	7.33	3.409	1.543	1.356	64.68		
22.00	1.1554	1.1575	254.2	2.592	901.2	97.0	272	1.3602	16.48	8.86	3.932	1.621	1.405	61.58		
24.00	1.1714	1.1735	281.1	2.866	890.3	108.0	298	1.3628	19.85	10.67	4.488	1.703	1.457	58.60		
26.00	1.1872	1.1893	308.7	3.147	878.5	119.7	323	1.3653	24.29	13.06		1.793	1.513	55.67		
28.00	1.2031	1.2052	336.9	3.435	866.2	132.0	347	1.3677	29.65	15.94		1.890	1.574	52.81		
30.00	1.2191	1.2213	365.7	3.729	853.4	144.9	371	1.3701	36.21	19.47		1.997	1.641	49.98		
32.00	1.2353	1.2375	395.3	4.030	840.0	158.2	395	1.3725	44.76	24.07		2.118	1.718	47.12		
34.00	1.2518	1.2540	425.6	4.339	826.2	172.1	419	1.3749	55.28	29.72		2.250	1.801	44.36		
36.00	1.2685	1.2707	456.7	4.656	811.8	186.4	443	1.3773				2.387	1.885	41.82		
38.00	1.2855	1.2878	488.5	4.981	797.0	201.2	467	1.3797				2.528	1.970	39.48		
40.00	1.3028	1.3051	521.1	5.313	781.7	216.5	491	1.3821				2.685	2.065	37.17		
42.00	1.3205	1.3229	554.6	5.655	765.9	232.3	516	1.3846				2.866	2.174	34.83		
44.00	1.3386	1.3410	589.0	6.005	749.6	248.6	540	1.3870				3.067	2.296	32.53		
46.00	1.3570	1.3594	624.2	6.365	732.8	265.4	565	1.3895				3.292	2.431	30.32		
48.00	1.3759	1.3783	660.4	6.734	715.5	282.8	590	1.3920				3.539	2.577	28.20		
50.00	1.3952	1.3977	697.6	7.113	697.6	300.6	616	1.3945				3.818	2.742	26.14		
52.00	1.4149	1.4174	735.8	7.502	679.2	319.1	641	1.3971				4.134	2.927	24.14		
54.00	1.4351	1.4377	775.0	7.901	660.2	338.1	667	1.3997				4.490	3.135	22.23		
56.00	1.4558	1.4584	815.3	8.312	640.6	357.7	694	1.4024				4.896	3.370	20.38		
58.00	1.4770	1.4796	856.7	8.734	620.3	377.9	720	1.4050				5.343	3.625	18.68		
60.00	1.4987	1.5013	899.2	9.168	599.5	398.8	747	1.4077				5.905	3.948	16.90		
62.00	1.5200	1.5227	942.4	9.608	577.6	420.6										
64.00	1.5421	1.5448	986.9	10.062	555.2	443.0										
66.00	1.5646	1.5674	1032.6	10.528	532.0	466.2										
68.00	1.5874	1.5902	1079.4	11.005	508.0	490.2										
70.00	1.6105	1.6134	1127.4	11.495	483.1	515.1										
72.00	1.6338	1.6367	1176.3	11.993	457.5	540.7										
74.00	1.6574	1.6603	1226.5	12.505	430.9	567.3										
76.00	1.6810	1.6840	1277.6	13.026	403.4	594.8										
78.00	1.7043	1.7073	1329.4	13.554	374.9	623.3										
80.00	1.7272	1.7303	1381.8	14.088	345.4	652.8										
82.00	1.7491	1.7522	1434.3	14.624	314.8	683.4										
84.00	1.7693	1.7724	1486.2	15.153	283.1	715.1										
86.00	1.7872	1.7904	1537.0	15.671	250.2	748.0										
88.00	1.8022	1.8054	1585.9	16.169	216.3	781.9										
90.00	1.8144	1.8176	1633.0	16.650	181.4	816.8										
92.00	1.8240	1.8272	1678.1	17.110	145.9	852.3										
94.00	1.8312	1.8344	1721.3	17.550	109.9	888.3										
96.00	1.8355	1.8388	1762.1	17.966	73.4	924.8										
98.00	1.8361	1.8394	1799.4	18.346	36.7	961.5										
100.00	1.8305	1.8337	1830.5	18.663	0.0	998.2										

Table 2

38 NITRIC ACID, HNO_3

MOLECULAR WEIGHT = 63.02
RELATIVE SPECIFIC REFRACTIVITY = 0.818

0.00 % by wt. data are the same for all compounds.
For Values of 0.00 wt. % solutions see Table 1, Acetic Acid.

A % by wt	ρ D_4^{20}	d D_{20}^{20}	C_v g/l	M g-mol/l	C_w g/l	$(C_w - C_v)$ g/l	$(n - n_d)$ $\times 10^4$	n	Δ °C	O Os/kg	S g-mol/l	η/η_w	$\eta\rho$ cS	ϕ rhe	γ mmho/cm	T g-mol/l
0.50	1.0009	1.0027	5.0	0.079	995.9	2.3	6	1.3336	0.281	0.151	0.080	1.002	1.003	99.64	28.4	0.323
1.00	1.0037	1.0054	10.0	0.159	993.6	4.6	13	1.3343	0.558	0.300	0.162	1.003	1.001	99.50	56.1	0.686
1.50	1.0064	1.0082	15.1	0.240	991.3	6.9	19	1.3349	0.837	0.450	0.244	1.004	1.000	99.40	84.7	1.10
2.00	1.0091	1.0109	20.2	0.320	988.9	9.3	26	1.3356	1.120	0.602	0.327	1.005	0.998	99.30	108.	1.50
2.50	1.0119	1.0137	25.3	0.401	986.6	11.7	32	1.3362	1.408	0.757	0.412	1.006	0.997	99.17	138.	1.97
3.00	1.0146	1.0164	30.4	0.483	984.2	14.0	39	1.3368	1.704	0.916	0.498	1.008	0.995	99.01	160.	2.57
3.50	1.0174	1.0192	35.6	0.565	981.8	16.5	45	1.3375	2.006	1.078	0.586	1.010	0.995	98.83	184.	3.18
4.00	1.0202	1.0220	40.8	0.648	979.4	18.9	51	1.3381	2.315	1.245	0.676	1.012	0.994	98.64	213.	4.31
4.50	1.0230	1.0248	46.0	0.730	976.9	21.3	58	1.3388	2.632	1.415	0.767	1.014	0.993	98.43		
5.00	1.0257	1.0276	51.3	0.814	974.5	23.8	64	1.3394	2.958	1.590	0.859	1.016	0.992	98.23		
5.50	1.0286	1.0304	56.6	0.898	972.0	26.3	71	1.3401	3.290	1.769	0.953	1.018	0.992	98.02		
6.00	1.0314	1.0332	61.9	0.982	969.5	28.7	78	1.3407	3.629	1.951	1.048	1.020	0.991	97.81		
6.50	1.0342	1.0360	67.2	1.067	967.0	31.3	84	1.3414	3.974	2.137	1.144	1.023	0.991	97.59		
7.00	1.0370	1.0389	72.6	1.152	964.4	33.8	91	1.3421	4.327	2.326	1.241	1.025	0.990	97.36		
7.50	1.0399	1.0417	78.0	1.238	961.9	36.3	97	1.3427	4.687	2.520	1.340	1.028	0.990	97.12		
8.00	1.0427	1.0446	83.4	1.324	959.3	38.9	104	1.3434	5.05	2.72	1.439	1.030	0.990	96.88		
8.50	1.0456	1.0475	88.9	1.410	956.7	41.5	110	1.3440	5.43	2.92	1.538	1.033	0.990	96.62		
9.00	1.0485	1.0504	94.4	1.497	954.1	44.1	117	1.3447	5.81	3.12	1.639	1.036	0.990	96.35		
9.50	1.0514	1.0533	99.9	1.585	951.5	46.7	124	1.3454	6.20	3.33	1.740	1.039	0.990	96.07		
10.00	1.0543	1.0562	105.4	1.673	948.9	49.4	130	1.3460	6.60	3.55	1.841	1.042	0.990	95.78		
10.50	1.0602	1.0620	116.6	1.850	943.5	54.7	144	1.3474	7.42	3.99	2.045	1.049	0.991	95.15		
11.00	1.0660	1.0679	127.9	2.030	938.1	60.1	157	1.3487	8.27	4.45	2.251	1.056	0.993	94.48		
11.50	1.0720	1.0739	139.4	2.211	932.6	65.6	170	1.3500	9.15	4.92	2.459	1.064	0.995	93.76		
12.00	1.0780	1.0799	150.9	2.395	927.1	71.2	184	1.3514	10.08	5.42	2.667	1.073	0.997	93.00		
12.50	1.0840	1.0859	162.6	2.580	921.4	76.8	198	1.3527	11.04	5.93	2.877	1.082	1.001	92.20		
13.00	1.0901	1.0921	174.4	2.768	915.7	82.5	211	1.3541	12.04	6.47	3.087	1.092	1.004	91.35		
13.50	1.0963	1.0982	186.4	2.957	909.9	88.3	225	1.3555	13.08	7.03	3.298	1.103	1.008	90.47		
14.00	1.1025	1.1044	198.4	3.149	904.0	94.2	239	1.3569	14.16	7.61	3.509	1.114	1.013	89.55		
14.50	1.1087	1.1107	210.7	3.343	898.0	100.2	253	1.3582	15.30	8.22	3.720	1.126	1.018	88.60		
15.00	1.1150	1.1170	223.0	3.538	892.0	106.2	266	1.3596				1.139	1.024	87.62		
15.50	1.1277	1.1297	248.1	3.937	879.6	118.6	294	1.3624				1.167	1.037	85.55		
16.00	1.1406	1.1426	273.7	4.344	866.8	131.4	322	1.3652				1.197	1.052	83.36		
16.50	1.1536	1.1557	299.9	4.759	853.7	144.6	350	1.3680				1.231	1.069	81.06		
17.00	1.1668	1.1688	326.7	5.184	840.1	158.1	378	1.3708				1.268	1.089	78.70		
17.50	1.1801	1.1822	354.0	5.618	826.0	172.2	406	1.3736				1.308	1.111	76.30		
18.00	1.1934	1.1955	381.9	6.060	811.5	186.7	433	1.3763				1.351	1.134	73.87		
18.50	1.2068	1.2090	410.3	6.511	796.5	201.7	460	1.3790				1.397	1.160	71.42		
19.00	1.2202	1.2224	439.3	6.970	780.9	217.3	487	1.3817				1.447	1.188	68.96		
19.50	1.2335	1.2357	468.7	7.438	764.8	233.5	513	1.3842				1.501	1.219	66.50		
20.00	1.2466	1.2489	498.7	7.913	748.0	250.2	537	1.3867				1.558	1.252	64.06		

Figure 2 Experimental Data for equilibrium freezing point (solid circles) and maximum supercooling (open circles) for increasing molality and known data from the Chemistry-Physics handbook (solid triangles) for ice-solution equilibrium point for H_2SO_4.

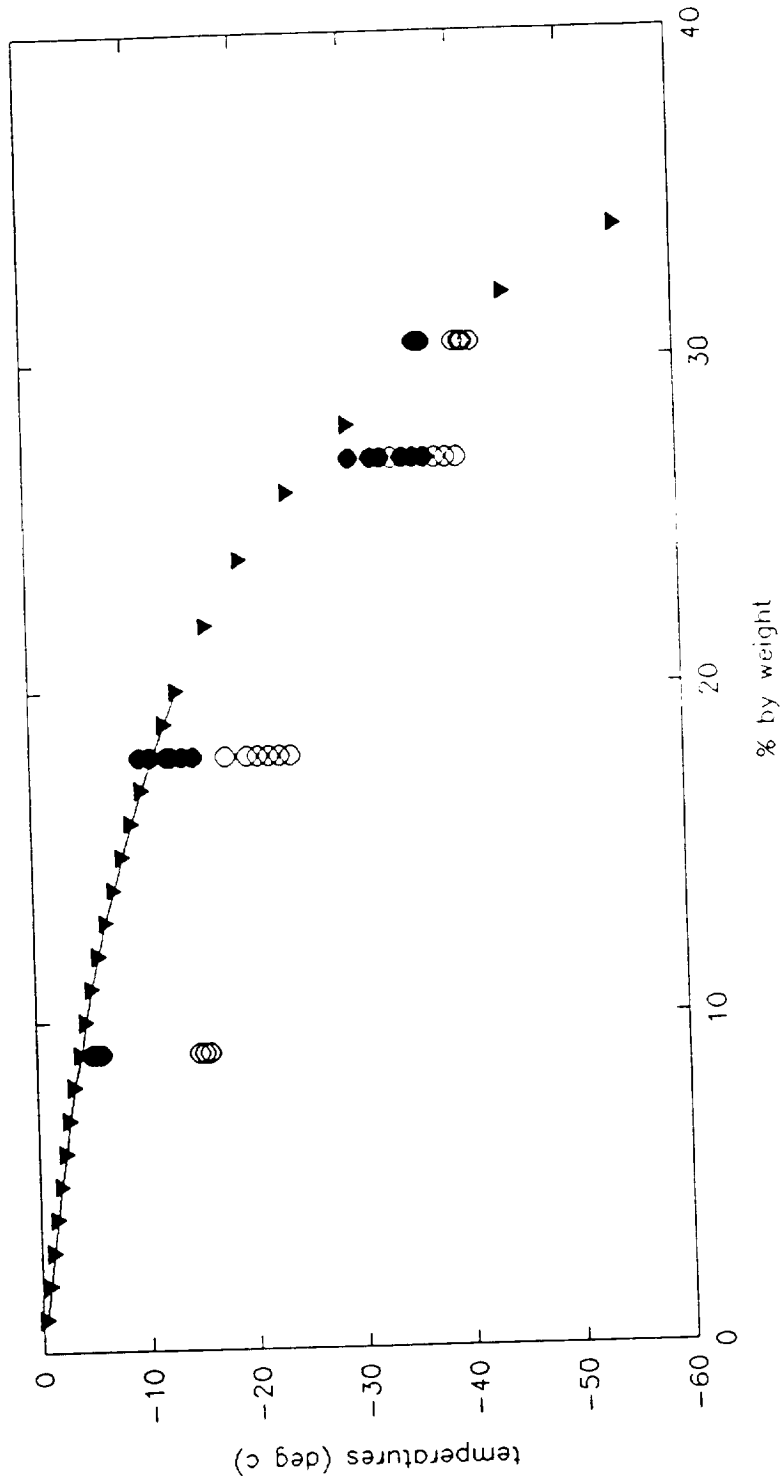

Figure 3. Same as Figure 2 for HNO_3.

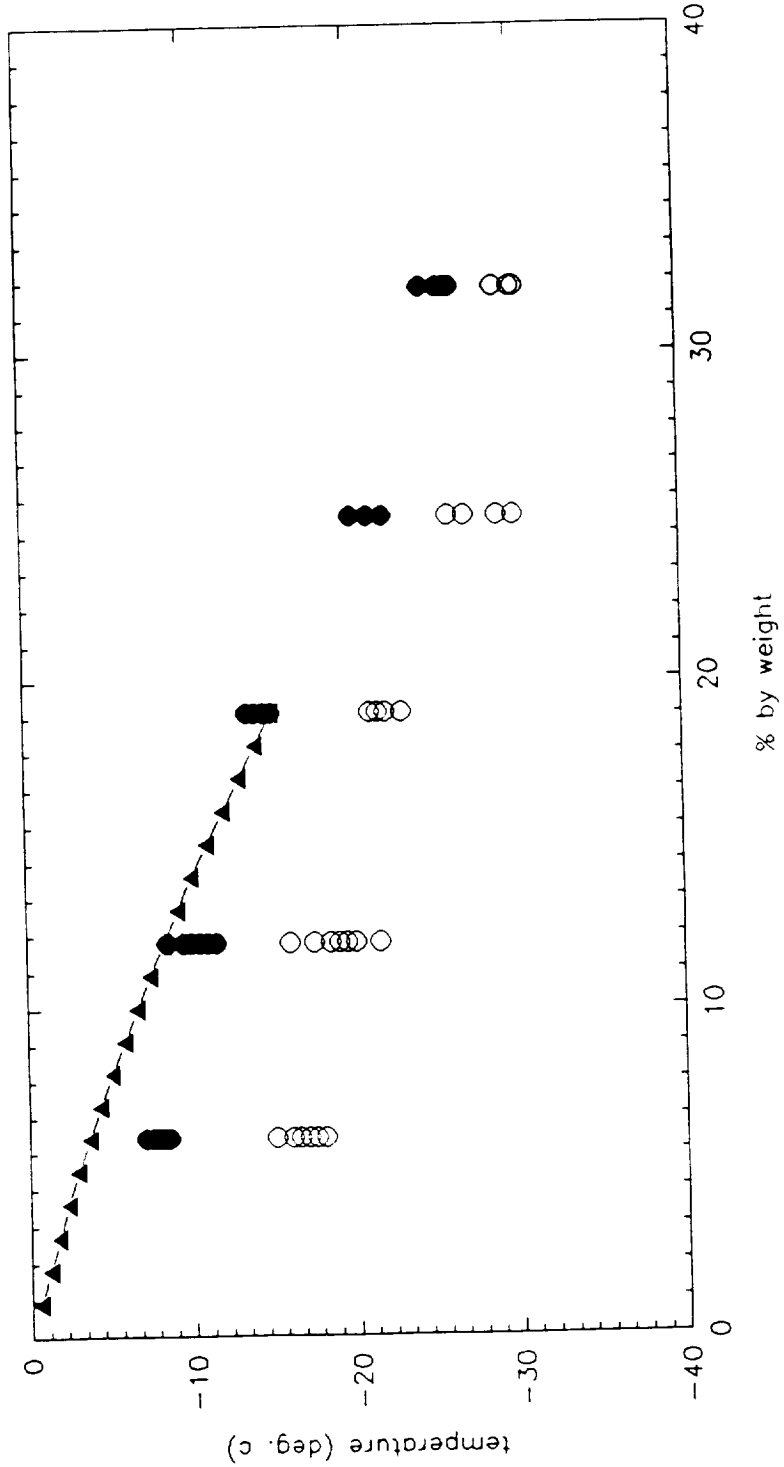

H_2SO_4, HNO_3. The maximum supercooling is represented by the open circles; it is demonstrated that there is a scatter of several degrees for each solution. The upper points (solid circles) represents the temperature reached by the solution within 1 to 5 s after the completion of the initial crystallization. This represents the equilibrium temperature of the solution after water has been removed by the crystallization, which enhances the concentration of the remaining solution. In the first instance we assume that the solid is pure ice, in which case all solute will be rejected, thus lowering the equilibrium melting point. The solution cools through equilibrium (A Fig. 4) to become supercooled (B) whereupon it nucleates to increase in temperature and solution concentration (C). This process is near adiabatic as the heat transfer to the environment is small over the times required for crystallization. Subsequently the mix cools to the bath temperature, more ice forms and the solution becomes more concentrated (D). E represents the ice eutectic. The amount of ice formed initially will be by given the expression:

$$\int_{T}^{Te} \frac{\sigma(T)\ dT}{L(T)}$$

where $\sigma(T)$ is the solution specific heat, L(T) the latent heat - neither of which are well known for the solutions under study.

A parallel study is to investigate how the crystals grow - particularly the linear growth velocity. This is readily accomplished by making a VCR tape of the propagation of the crystallization front after nucleating the solution at a prescribed supercooling. The velocity is measured directly from the tape.

Figure 4: Schematic of conditions for nucleation of a supercooled solution. Arrows indicate solution temperature as it is cooled through the equilibrium point (A), nucleates at substantial supercooling (B) grows crystals adiabatically and concentrates (C) and finally equilibrates at the environmental temperature (D). The diagram beyond E (the ice - eutectic) represents the conditions for a hydrate which can experience the same process either side of the congruent melting point (MP).

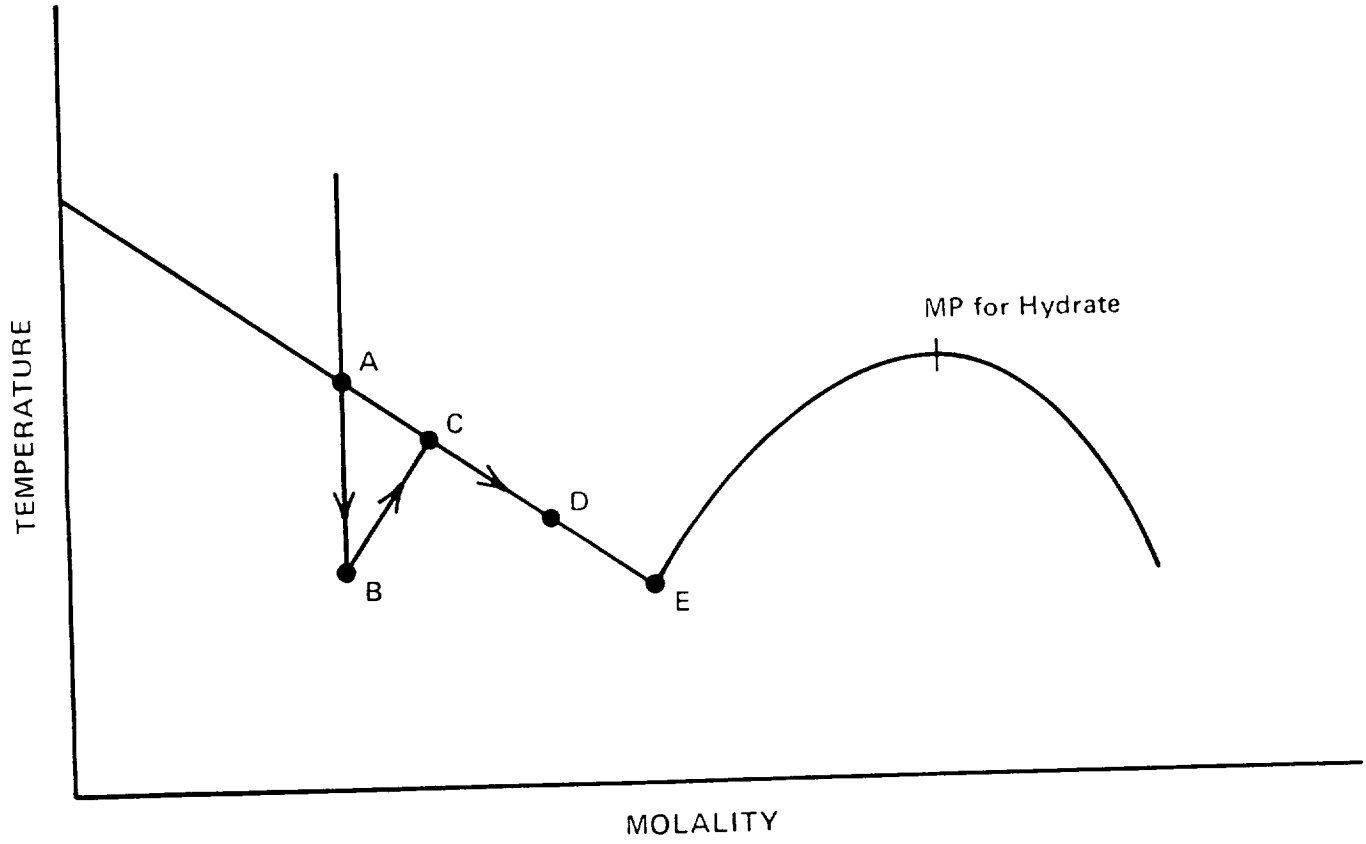

For these solutions the viscosity increases substantially with decrease of temperature. At sufficiently low temperature; the growth velocity decreases until crystallization ceases. Figure 5 shows preliminary measurements; Figure 6 shows schematic of anticipated results from cruder qualitative measurements. This shows that a glass has formed. The results indicate that this happen for both acids under appropriate conditions. The above arguments all apply in the region of hydrate formation (i.e. to right of point E in Fig. 4), data in these regions is required.

2. Diffusion Chamber

Work is underway on the design and construction of a diffusion chamber to study aerosol and crystal growth directly (Fig. 7), temperature control will be by circulating bath and surface heater; the upper plate moisture/acid vapor source will be made of acid resistant stainless steel. The chamber walls will be made of acid resistant plastic. Temperature range, -90 to -60°C. Crystals will grow as indicated and examined by VCR; external aerosol will be injected as appropriate and examined for phase change (optical twinkling).

Figure 5. Measurements of ice crystal growth velocity in various molality of H_2SO_4 solutions. Degrees supercooling as for pure water below °C.

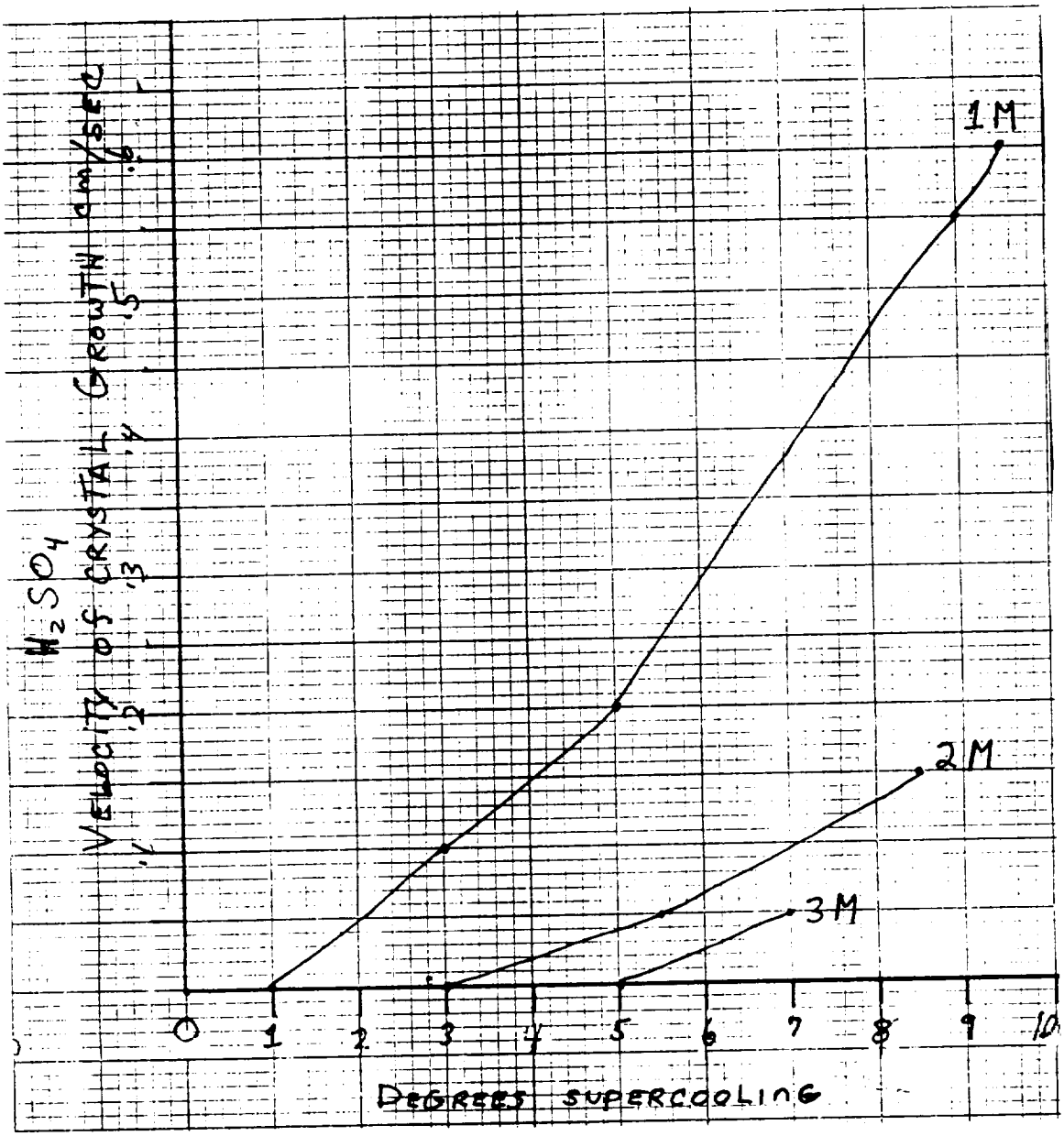

Figure 6: Schematic of crystal growth velocity for H_2SO_4 solution characterizes the glass transition where V = zero, other than at the equilibrium melting point at high supercooling and high molality.

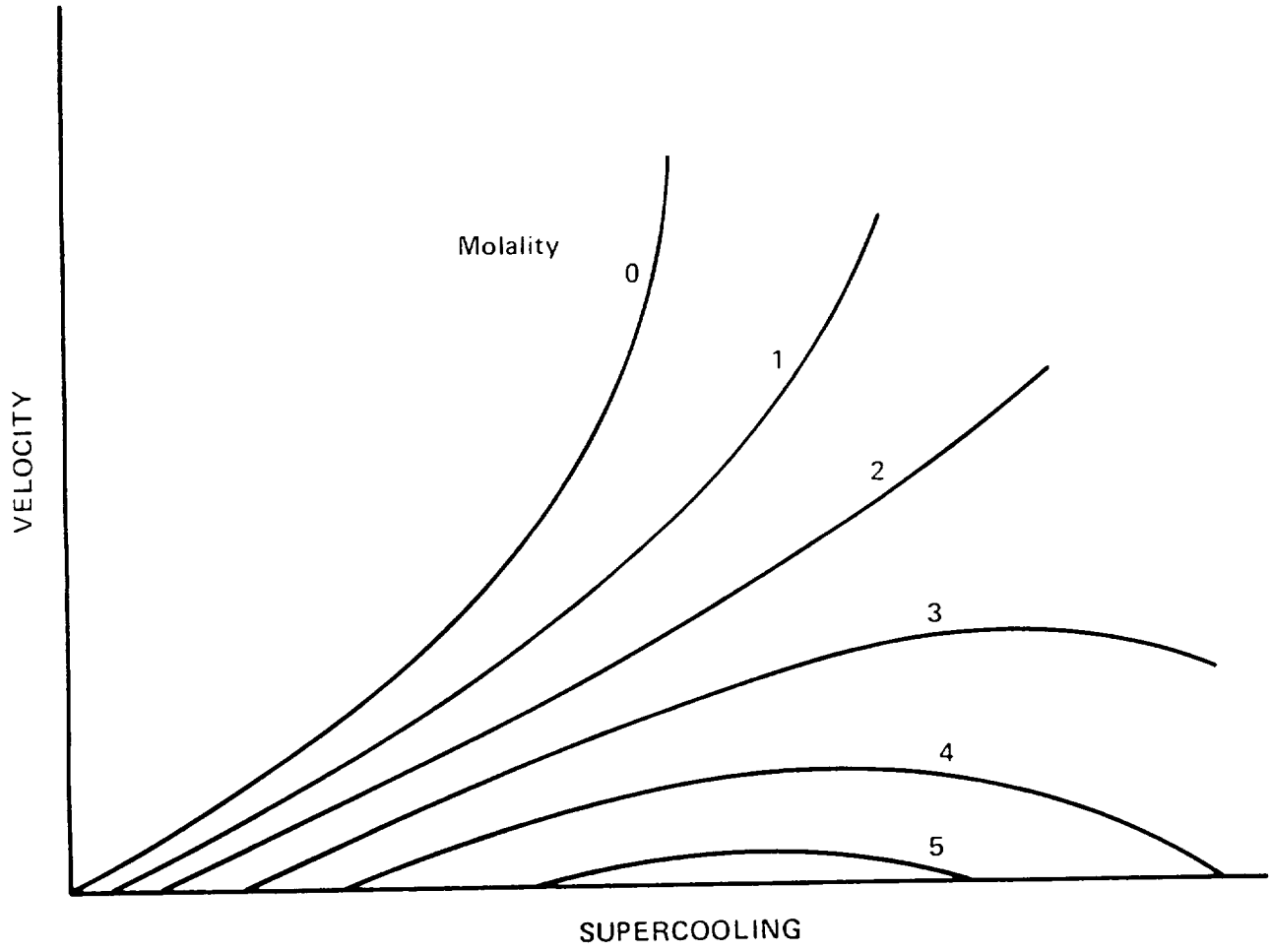

Figure 7: Diffusion chamber schematic. The walls are designed to withstand acid; the moisture source contains appropriate acid solution. The temperatures of top and bottom plates determine the mid temperature, the difference determines the mid level supersaturation. Crystals grow from the vapor on the central sting; otherwise aerosol is used from an outside source.

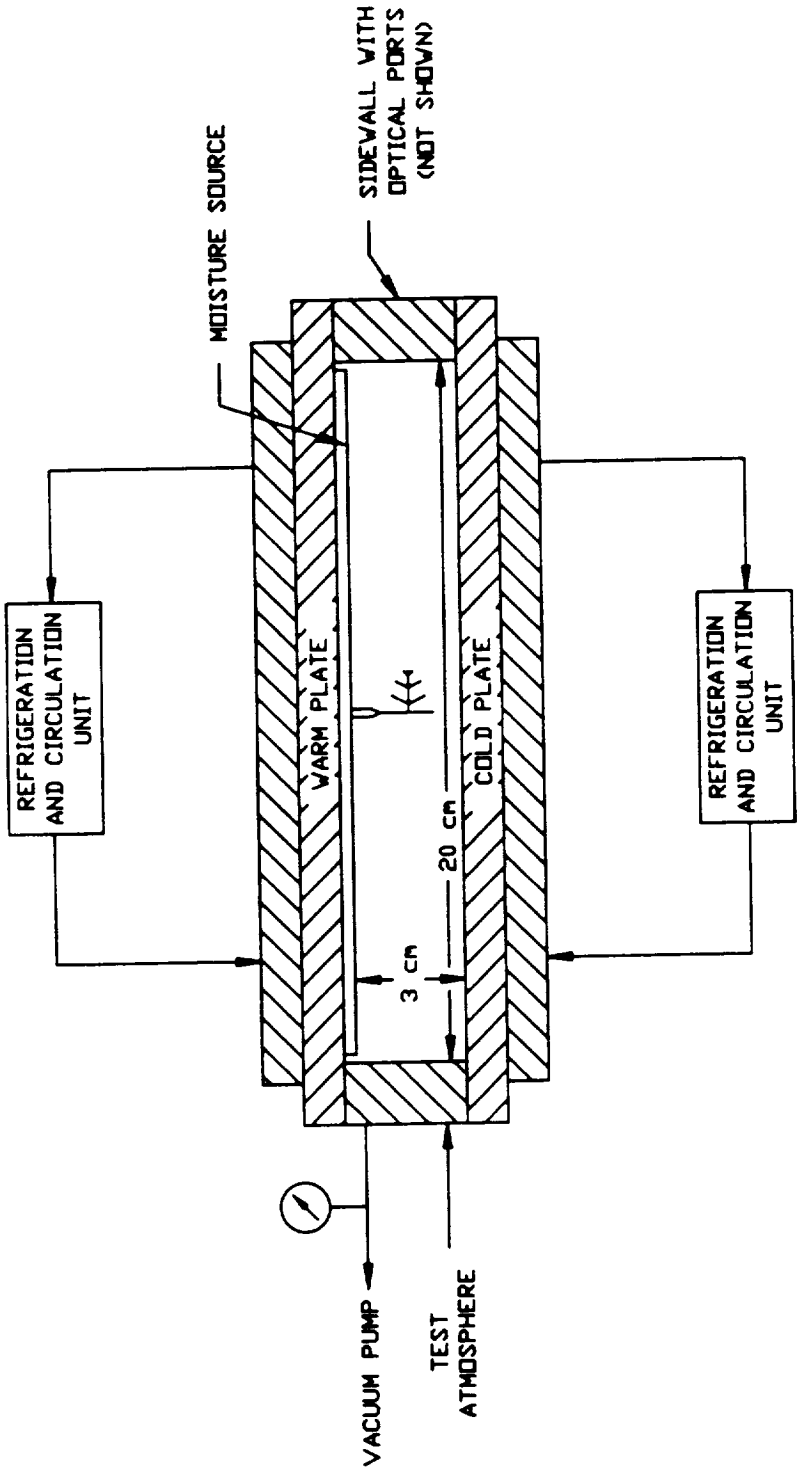

3. Initial Conclusions

The existence of the potential for substantial supercooling and a glass transition in polar stratospheric cloud particles opens new possibilities for surface chemistry. It would appear that the supercooled solutions might be less effective for a chemical reactions since the molecules would be more likely to enter the body of the solution. This will however depend on the self diffusion, which will fall as any glass transition is approached.

Equally important is that aerosol which is cycled through colder to warmer temperatures (as opposed to aerosol which goes from warmer to colder temperatures) will be more likely to form ice as hydrate clouds, since the glass will crystallize as its temperature is increased. Thus the behavior of a particle and its response to subsequent chemical reactions and cloud formation as it cools radiatively or by mountain were lifting may be determined by its previous history.

4. Continuing Work

- Repeat the supercooling experiments with smaller volumes (mm^3) to reach lower supercooling; extrapolate results to small aerosol values (μm)
- Explore the range of glass transition and measure growth velocities in greater detail, together with crystal shape.
- Examine the role of impurities (soot) on maximum supercooling.
- Extend studies to hydrate regions.
- Complete diffusion chamber and examine vapor growth in hydrate region.

5. References

Mason, B. J., 1970: Physics of Clouds, Oxford 1970.

Hallett, J. and J.G. Hudson, 1991: Stratospheric Soot: Cloud forming properties and transport processes. AIAA/AHS/ASEE Aircraft Design Systems and Operations Meeting, Harbor, Baltimore, MD. AIAA 9th Applied Aerodynamics Conference, September 23-25, 1991.